Regulation of the Cardiac Na^+-Ca^{2+} Exchanger by the Endogenous XIP Region

Satoshi Matsuoka,* Debora A. Nicoll,‡|| Zhaoping He,‡|| and Kenneth D. Philipson‡||§

From the *Department of Physiology, Faculty of Medicine, Kyoto University, Sakyo-ku, Kyoto 606-01, Japan; and ‡Department of Physiology, §Department of Medicine, and ||Cardiovascular Research Laboratories, University of California at Los Angeles, School of Medicine, Los Angeles, California 90095-1760

ABSTRACT The cardiac sarcolemmal Na^+-Ca^{2+} exchanger is modulated by intrinsic regulatory mechanisms. A large intracellular loop of the exchanger participates in the regulatory responses. We have proposed (Li, Z., D.A. Nicoll, A. Collins, D.W. Hilgemann, A.G. Filoteo, J.T. Penniston, J.N. Weiss, J.M. Tomich, and K.D. Philipson. 1991. *J. Biol. Chem.* 266:1014–1020) that a segment of the large intracellular loop, the endogenous XIP region, has an autoregulatory role in exchanger function. We now test this hypothesis by mutational analysis of the XIP region. Nine XIP-region mutants were expressed in *Xenopus* oocytes and all displayed altered regulatory properties. The major alteration was in a regulatory mechanism known as Na^+-dependent inactivation. This inactivation is manifested as a partial decay in outward Na^+-Ca^{2+} exchange current after application of Na^+ to the intracellular surface of a giant excised patch. Two mutant phenotypes were observed. In group 1 mutants, inactivation was markedly accelerated; in group 2 mutants, inactivation was completely eliminated. All mutants had normal Na^+ affinities. Regulation of the exchanger by nontransported, intracellular Ca^{2+} was also modified by the XIP-region mutations. Binding of Ca^{2+} to the intracellular loop activates exchange activity and also decreases Na^+-dependent inactivation. XIP-region mutants were all still regulated by Ca^{2+}. However, the apparent affinity of the group 1 mutants for regulatory Ca^{2+} was decreased. The responses of all mutant exchangers to Ca^{2+} application or removal were markedly accelerated. Na^+-dependent inactivation and regulation by Ca^{2+} are interrelated and are not completely independent processes. We conclude that the endogenous XIP region is primarily involved in movement of the exchanger into and out of the Na^+-induced inactivated state, but that the XIP region is also involved in regulation by Ca^{2+}.

KEY WORDS: Na^+-Ca^{2+} exchange • exchanger inhibitory peptide • mutagenesis • giant excised patch

INTRODUCTION

The sarcolemmal Na^+-Ca^{2+} exchanger is the primary Ca^{2+} extrusion mechanism in cardiac myocytes and has a central role in regulating myocardial contractility. The exchanger has been cloned (Nicoll et al., 1990) and is modeled to consist of two groups of transmembrane segments separated by a large intracellular loop. The intracellular loop is over 500 amino acids in length but is not essential for transport function. The loop, however, has been shown to be involved in the regulation of Na^+-Ca^{2+} exchange activity (Matsuoka et al., 1993; Matsuoka et al., 1995).

The exchanger is subject to two forms of intrinsic regulation designated I_1 and I_2 (Hilgemann et al., 1992*a,b*). I_1 was first observed by Hilgemann (1990) and has also been termed Na^+-dependent inactivation. Na^+-dependent inactivation is manifested as a partial inactivation of outward exchange current upon application of Na^+ to the intracellular surface.

Address correspondence to D. Nicoll, Cardiovascular Research Laboratory, MRL 3645, 675 Circle Drive South, Los Angeles, CA 90095-1760. Fax: 310-206-5777; E-mail: debora@cvrl.ucla.edu

I_2, also termed Ca^{2+}-dependent regulation, was first described in the squid axon (DiPolo, 1979). The exchanger is regulated by intracellular Ca^{2+} at a high affinity binding site which is distinct from the Ca^{2+} transport site. Regulatory Ca^{2+} is not transported. Binding of regulatory Ca^{2+} activates Na^+-Ca^{2+} exchange activity with an apparent K_D of 0.2–0.4 μM (Matsuoka et al., 1995) although this measurement is dependent on experimental conditions. The binding site for regulatory Ca^{2+} has been identified on a central region of the large intracellular loop (Levitsky et al., 1994; Matsuoka et al., 1995).

Regulation by both Na^+ and Ca^{2+} are most readily studied using the giant excised patch technique (Hilgemann, 1989). Thus, for example, with a membrane patch in the inside-out configuration and with Ca^{2+} in the pipette, rapid addition of Na^+ to the bath initiates an outward Na^+-Ca^{2+} exchange current; the current rapidly peaks and then decays, due to Na^+-dependent inactivation, to a steady-state level. The decay occurs over several seconds. The inactivated state of the exchanger is modeled to form after Na^+ binds to the intracellular transport site of the protein. Three Na^+ ions bind to the transport site and either induce transloca-

tion of the ions across the membrane or induce a fraction of the exchangers to enter an inactivated state (Hilgemann et al., 1992*b*). Although the intracellular loop of the exchanger has been implicated in Na^+-dependent inactivation (Matsuoka et al., 1993), no specific molecular information is available on the origin of the inactivation process.

A portion of the intracellular loop of interest is known as the endogenous XIP region (Li et al., 1991). This region is comprised of 20 amino acids at the amino terminus of the loop immediately following the fifth transmembrane segment. It was proposed that the endogenous XIP region might have an autoregulatory function. Exogenously added peptide, with the XIP sequence, potently inhibits exchange activity, consistent with this proposal.

In this study, we investigated the role of the endogenous XIP region in the Na^+-Ca^{2+} exchange process using site-directed mutagenesis. Mutant exchangers were expressed in *Xenopus* oocytes and analyzed using the giant excised patch technique. We find that the endogenous XIP region plays a central role in the Na^+-dependent inactivation process and is also involved in Ca^{2+}-dependent regulation.

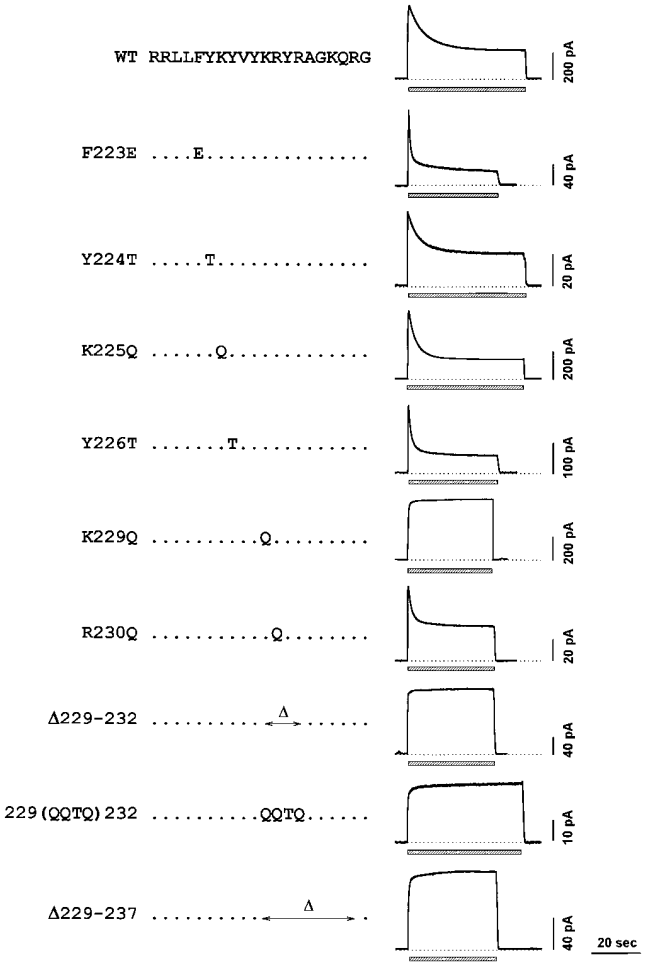

FIGURE 1. XIP region mutations in the Na^+-Ca^{2+} exchanger and the outward Na^+-Ca^{2+} exchange current of the mutants. The amino acid sequence of the XIP region for the wild-type exchanger (*WT*) is shown as one-letter abbreviations. For the mutants, dots show unchanged amino acids and arrows indicate deleted regions. The outward Na^+-Ca^{2+} exchange currents of the wild-type and XIP region mutant exchangers were induced by replacing 100 mM Cs^+ with 100 mM Na^+ at the cytoplasmic face of the patch (*bars*). Extracellular and cytoplasmic Ca^{2+} were 8 mM and 1 μM, respectively. Dotted lines indicate 0 current level.

METHODS

Preparation of Mutant Na^+-Ca^{2+} Exchangers

Mutations in the wild-type exchanger were generated as described previously (Nicoll et al., 1996) using the Sculptor in vitro mutagenesis kit (Amersham Corp., Arlington Heights, IL). cRNA was synthesized with mCAP mRNA capping kit (Stratagene Inc., La Jolla, CA) after linearization with Hind III. The cRNA (5 ng, 50 nl) was injected into *Xenopus laevis* oocytes which had been prepared as previously described (Longoni et al., 1988). The Na^+-Ca^{2+} exchange currents were measured after incubation for 3–6 d at 17–19°C. The mutations which were generated for this series of experiments are summarized in Fig. 1.

Two types of mutations were constructed. Initially, deletions to the COOH-terminal region of XIP tested the effects of gross mutations. Subsequently, single-site substitutions were made. Basic and aromatic residues were targeted since parallel experiments involving amino acid substitutions in the XIP peptide indicate the importance of these residues in exchanger inhibition (He et al., 1997). Basic residues were changed to neutral, hydrophilic glutamine residues and aromatic tyrosines were changed to threonine to eliminate the aromatic but maintain the hydroxyl characteristics of the residue. In one case, the aromatic residue F223, in the highly conserved NH_2-terminal portion of the endogenous XIP region, was mutated to glutamate to eliminate the aromatic group and introduce an acidic residue into a basic region of the exchanger. All mutations to the XIP region resulted in functional exchangers, and all mutations which were constructed are discussed in the following text.

Experimental Solutions

Pipette (extracellular) and bath (cytoplasmic) solutions were essentially the same as described (Matsuoka et al., 1995). All pipette solutions contained (in mM) CsOH (20), $Mg(OH)_2$ (2), TEA-OH (20), HEPES (20), ouabain (0.25), and MES (100). To measure outward exchange currents, the pipette solution also contained 8 mM $CaCO_3$ and 100 mM *N*-methyl-D-glucamine (NMG). To measure both outward and inward currents in the same patch, the pipette solution also contained 2 mM $CaCO_3$ and 140 mM NaOH. The pH was adjusted to 7.0 with MES. 0.1 mM Niflumic acid (Sigma Chemical Co., St. Louis, MO; 200 mM stock solution in DMSO) was included to suppress the endogenous Ca^{2+}-activated Cl^- current (White and Aylwin, 1990).

The bath solutions contained CsOH (20), NaOH and/or CsOH (100), EGTA (10), $CaCO_3$ (0-10), $Mg(OH)_2$ (1–1.5), TEA-OH (20), HEPES (20), and MES (100). pH was adjusted to 7.0 with MES. Free Ca^{2+} and Mg^{2+} concentrations were calculated using MAXC software (Bers et al., 1993). The free Ca^{2+} concentration was 1 μM unless otherwise noted in the text or figure legend. Free Mg^{2+} concentration was 1 mM in all cytoplasmic solutions.

Electrophysiological Studies

The Na^+-Ca^{2+} exchange current was measured using the inside-out giant patch method (Matsuoka et al., 1993). Oocytes were first placed in a hyperosmotic solution [(in mM): KOH (100), MES (100), HEPES (20), EGTA (5), $Mg(OH)_2$ (5), K-aspartate (100) or mannitol (200), pH adjusted to 7.0 with MES] for 5–10 min. The vitellin layer was then manually removed with forceps. The oocytes were transferred to a bath solution identical to the hyperosmotic solution but lacking K-aspartate or mannitol, for seal formation.

Borosilicate glass (O.D. 1.65 mm and I.D. 1.32 mm; Hilgenberg GmbH, Malsfeld, Germany) was used for giant patch experiments. Pipettes with tip diameters of 20–35 μm were prepared by the method developed by Hilgemann (Hilgemann, 1989) and coated with a parafilm (American National Can, Greenwich, CT)-light mineral oil (Sigma Chemical Co.) mixture (Matsuoka et al., 1995). Heavy mineral oil (Sigma) or decane (Wako Pure Chemical Industries, Osaka, Japan) was occasionally added to the mixture to stabilize the patch.

Membrane currents were measured using EPC-7 (HEKA Elektronik, Lambrecht, Germany) or Axopatch 200A (Axon Instruments, Inc., Foster City, CA) and filtered at 1 kHz by a lowpass filter (NF Electronic Instruments, Yokohama, Japan). Membrane currents were recorded by a personal computer (Epson PC-486SE, Tokyo, Japan) with 12 bit DMA A/D converter (Canopus ADX-98H, Japan: sampling frequency was 50 Hz). For current-voltage (I-V) relation measurements, a ramp pulse was generated by a function generator (FG-122, NF Electronic Instruments), and membrane current and voltage were recorded by another computer (NEC PC-9821AP2, Japan) with the same A/D converter. Sampling frequency was 2,500 Hz.

All experiments were carried out at 30°C. Data are shown as mean ± SD.

RESULTS

The Outward Na^+-Ca^{2+} Exchange Current from XIP-region Mutants

Outward Na^+-Ca^{2+} exchange currents were induced by applying Na^+ to the cytoplasmic side of inside-out patches excised from oocytes expressing the cloned cardiac exchanger, NCX1. Representative outward currents from wild type and each XIP-region mutant exchanger are shown in Fig. 1. Current levels varied considerably from patch to patch and ranged from 20 to 500 pA. For the wild-type (WT)[1] exchanger, Na^+-dependent inactivation (I_1; Hilgemann et al., 1992*b*), can be seen as a time-dependent decline of outward current during Na^+ application.

All mutant exchangers were active, displaying an outward Na^+-Ca^{2+} exchange current upon application of cytoplasmic Na^+ (Fig. 1). However, with respect to Na^+-dependent inactivation, the mutants fall into two groups. Group 1 consists of mutants F223E, Y224T, K225Q, Y226T, and R230Q, which display a Na^+-dependent inactivation. Group 2 consists of mutants K229Q, Δ229–232, 229(QQTQ)232, and Δ229–237 which do not display a current decay.

A measure of the extent of Na^+-dependent inactivation is Fss, the ratio of steady state to the initial exchanger current. The quasi-steady state current was measured 36–48 s after application of 100 mM Na^+, and the initial current was measured either at the peak (for group 1 mutants) or at ~2 s after Na^+ application (for group 2 mutants). The calculated Fss for each mutant and wild-type Na^+-Ca^{2+} exchanger is shown in Table I.

In group 2 mutants (shaded), Fss values are significantly larger than for the wild type. The Fss for the wild-type exchanger is ~0.4 while for mutants K229Q, Δ229–232, 229(QQTQ)232, Δ229–237 it is about 1. This reflects the lack of any observable Na^+-dependent inactivation in these mutants (Fig. 1).

In group 1 mutants, the Fss more closely approximates that of the wild-type exchanger (Fig. 1). However, for mutants F223E and Y226T, Fss is significantly smaller than for the wild type, reflecting a greater extent of inactivation.

Altered Kinetics of Na^+-dependent Inactivation in Group 1 Mutants

$T_{1/e}$ (the 1/e time for the current to decay from peak to steady state) was determined for each group 1 mutant (Table II). Each of the group 1 mutants displayed a significant decrease in $T_{1/e}$. Hence, the rate of the Na^+-dependent inactivation was increased in the group 1 XIP region mutants.

The kinetics of the Na^+-dependent inactivation was examined in more detail by exponentially fitting the current decay. Fig. 2 demonstrates two-exponential fittings of the wild-type and F223E currents after subtraction of the quasi-steady state component (36–48 s after 100 mM Na^+ application). In the examples shown, the time constants of the fast components (τ_{fast}) were 2.5 s for wild type and 0.6 s for F223E, and the time con-

TABLE I

Current Decay in XIP Region Mutants

Mutant	Fss	*n*
Wild-type	0.4 ± 0.1	14
F223E	0.2 ± 0.1*	8
Y224T	0.3 ± 0.1	6
K225Q	0.3 ± 0.1	9
Y226T	0.2 ± 0.1*	7
K229Q	1.0 ± 0.1*	12
R230Q	0.5 ± 0.2	12
Δ229–232	1.0 ± 0.1*	13
229(QQTQ)232	1.1 ± 0.1*	8
Δ229–237	1.1 ± 0.1*	7

The extent of current decay, Fss, was measured during 100 mM Na^+ application. Fss is the ratio of the exchange current at steady state to the current at peak. Mutants that belong to group 2 are shaded. *$P < 0.01$.

[1]*Abbreviations used in this paper:* Fss, ratio of steady state to the initial exchanger current; WT, wild type.

TABLE II

Rate of Na^+-dependent Inactivation in Group 1 Mutants

Mutant	$T_{1/e}$	
	s	
Wild-type	8.9 ± 2.3	(13)
F223E	1.3 ± 0.5*	(8)
Y224T	3.3 ± 0.8*	(6)
K225Q	4.9 ± 0.8*	(9)
Y226T	2.0 ± 0.3*	(7)
R230Q	1.9 ± 0.5*	(13)

*$P < 0.01$; *n* is given in parentheses.

stants of the slow components (τ_{slow}) were 7.9 s for the wild type, and 10.0 s for F223E.

Table III summarizes the results of two-exponential fitting for each of the group 1 mutants. For K225Q, τ_{fast} was similar to the wild type and, for the other mutants, τ_{fast} was smaller than that of the wild type, especially for F223E. On the other hand, the τ_{slow} values of all group 1 mutants are similar to that of the wild-type exchanger.

For the wild-type Na^+-Ca^{2+} exchanger, the ratio of the amplitude of the fast component to the slow component (I_{fast}/I_{slow}) was <1 (0.3 ± 0.2) and in all group 1 mutants, the amplitude ratio was >1 (between 1.3 and 4.7), resulting in a dominance of the fast component in the mutants. Hence, in group 1 mutants the fast component is somewhat faster and much more dominant while the rate of the slow component appears to be unaffected by the mutations. The result is an acceleration of the Na^+-dependent inactivation relative to wild type.

In 6 out of 14 patches of the wild-type exchanger, 3 out of 9 patches of K225Q, and 7 out of 13 patches of R230Q, one exponential could fit the inactivation. In these patches, the wild type could be fit with a single τ_{slow}-like time constant of 11.3 ± 2.3 s, the K225Q mutant with an intermediate τ of 5.5 ± 1.1 s, and the R230Q mutant with a τ_{fast}-like time constant of 1.7 ± 0.5 s. These results are consistent with the observed τ_{slow} dominance of the wild-type inactivation, the near equivalence of τ_{slow} and τ_{fast} in the K225Q mutant and the τ_{fast} dominance in the R230Q mutant (Table III).

Transport Cycle Na^+-dependence of XIP Region Mutants

Varying the intracellular Na^+ concentration used to elicit exchange current for the wild-type Na^+-Ca^{2+} exchanger has two primary effects (Hilgemann et al., 1992*b*; Fig. 3). First, the peak exchange current is elevated at higher levels of Na^+. Second, the extent of inactivation (as seen by the decrease in Fss) increases as Na^+ concentration is raised. This has been modeled by Hilgemann et al.(1992*b*) to imply that the exchanger enters the inactive state via the state in which three Na^+ ions are bound to the intracellular transport sites. The instantaneous current, which is measured before a significant level of Na^+-dependent inactivation occurs, is related to the affinity of the exchanger for transported Na^+.

Fig. 3 demonstrates representative current traces from the wild-type exchanger, mutants Y224T (group 1) and K229Q (group 2), at 6–100 mM cytoplasmic Na^+. Also shown is a control with water-injected oocytes at 100 mM Na^+. Little or no current was observed in the water-injected cells. At the lowest Na^+ concentration studied, 6 mM, a small but significant outward current was observed for each of the Na^+-Ca^{2+} exchangers. However, there was very little current decay. An in-

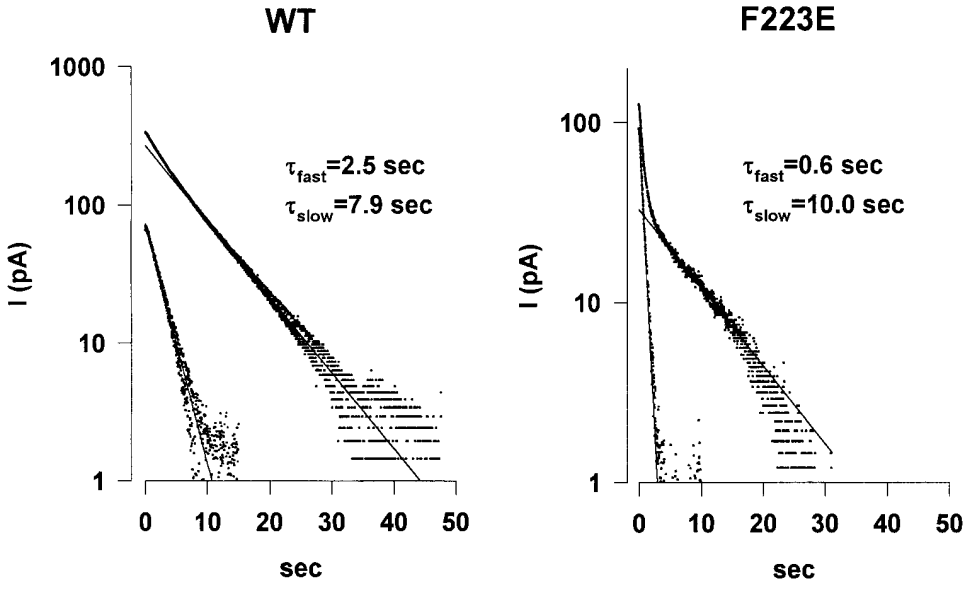

FIGURE 2. Fitting the Na^+-dependent inactivation to two exponentials; examples for the wild-type (*WT*) and mutant F223E exchangers. The slow component (*right-most dotted curve*) was first fit by the least square method after subtracting the steady state component. The solid line through the data points corresponds to the fitted slow component. The intercept of the fitted line with the ordinate is a measure of I_{slow}. After the slow component was fit, it was subtracted from the current trace, and the remaining current was fit by a second exponential (*left-most dotted curve*). The solid line through those data points corresponds to the fitted fast component and the intercept of that line with the ordinate corresponds to the magnitude of I_{fast}.

TABLE III

Summary of 2-exponential Fitting of Group 1 Mutants

Mutant	τ_{fast}	τ_{slow}	I_{fast}/I_{slow}	*n*
	s	*s*		
Wild-type	2.4 ± 0.8	9.4 ± 2.7	0.3 ± 0.2	8
F223E	0.7 ± 0.1‡	10.7 ± 2.4	3.6 ± 1.5‡	8
Y224T	1.8 ± 0.4*	12.2 ± 3.0	2.4 ± 1.7*	6
K225Q	2.4 ± 0.4	9.8 ± 1.1	1.3 ± 0.2‡	6
Y226T	1.3 ± 0.2‡	10.7 ± 1.6	3.5 ± 0.8‡	7
R230Q	1.4 ± 0.2‡	11.9 ± 4.5	4.7 ± 2.4‡	6

Data column 1 (τ_{fast}) and data column 2 (τ_{slow}) were determined as described in Fig. 2. Data column 3 (I_{fast}/I_{slow}) was determined from the intercepts of the fitted lines with the ordinate as shown in Fig. 2. *$P < 0.05$, ‡$P < 0.01$ compared to wild-type.

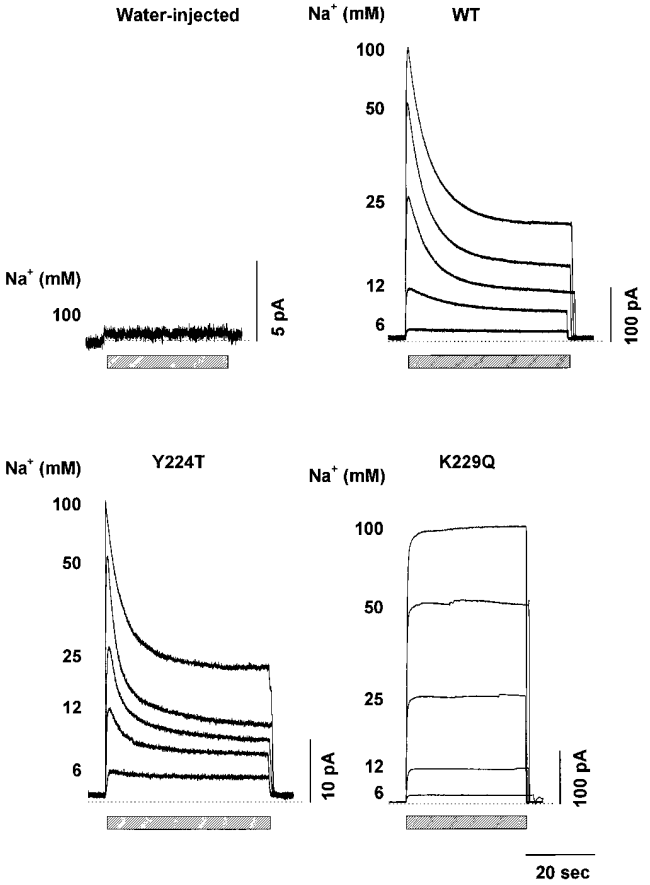

FIGURE 3. Outward Na^+-Ca^{2+} exchange currents at different cytoplasmic Na^+ concentrations are shown for the wild type (*WT*) and representatives of group 1 (*Y224T*) and group 2 mutants (*K229Q*) and water-injected cells. Cytoplasmic Na^+ concentrations were 6, 12, 25, 50, and 100 mM from the lower trace to the upper trace for all exchangers. The period of Na^+ application is indicated by the crosshatched bar. Dotted lines indicate 0 current level.

crease of cytoplasmic Na^+ from 6 to 100 mM augmented the outward current amplitude of all three exchangers and enhanced the Na^+-dependent inactivation in the wild-type and Y224T exchangers. This tendency was also observed in other group 1 mutants. No obvious current decay was observed in K229Q or other group 2 mutants in the range of 6 to 100 mM cytoplasmic Na^+.

The apparent half-maximal concentration (K_h) for Na^+ transport was determined for the wild-type and each mutant Na^+-Ca^{2+} exchanger (Fig. 4). Peak currents at each Na^+ concentration were normalized to the peak current at 100 mM Na^+ and then plotted as a function of Na^+ concentration. The Na^+ concentration-current relationship of K225Q (group 1) and 229(QQTQ)232 (group 2) were superimposable with that of the wild-type exchanger. The other mutants behaved similarly (Table IV, 1st data column) and no differences in $K_h(Na^+)$ were observed. These data demonstrate that the Na^+ affinity of the transport cycle is unchanged in the XIP region mutants.

The basic properties of the transport cycle were further studied by measuring the steady-state current-voltage (I-V) relation. In oocytes expressing mutant exchangers, the voltage dependencies of outward currents induced by 100 mM Na^+ were almost identical to wild type (data not shown). Since the voltage dependence of the exchanger has been attributed to the Na^+ and/or Ca^{2+} translocation steps in the transport cycle (Hilgemann et al., 1991; Niggli and Lederer, 1991; Matsuoka and Hilgemann, 1992), it is concluded that the basic properties of the transport cycle are intact in all XIP region mutants.

Na^+ Dependence of Na^+-dependent Inactivation

To determine the Na^+ dependence of Na^+-dependent inactivation, Fss, a measure of the amount of Na^+-dependent inactivation, was plotted as a function of intracellular Na^+ concentration for wild type and two of the group 1 mutants (Fig. 5 *A*) and for group 2 mutants (Fig. 5 *B*). In the wild-type and group 1 mutant exchangers, the Fss values decrease as Na^+ increases from 6 to 25 mM. That is, inactivation becomes more prominent as Na^+ increases. The saturation point was reached at 25 to 50 mM. Beyond 50 mM Na^+, Fss tends to increase slightly (e.g., Fig 5 *A*, *WT*).

Data for the wild-type and group 1 mutants were fit to a modified Hill equation, assuming Fss to be 1.0 in the absence of Na^+. Average $K_h(Na^+)$ values ranged from 6 to 12 mM (Table IV, 2nd data column) and differences from the wild type were small. Therefore, the apparent Na^+ affinity of the Na^+-dependent inactivation is relatively unaffected by mutations in the XIP region. It is notable that the $K_h(Na^+)$ values for F_{ss} are lower than for I_{peak} (Table IV). This result is consistent with previous modeling and experimental data (Hilgemann et al., 1992*b*). In the model of Hilgemann et al., it is as-

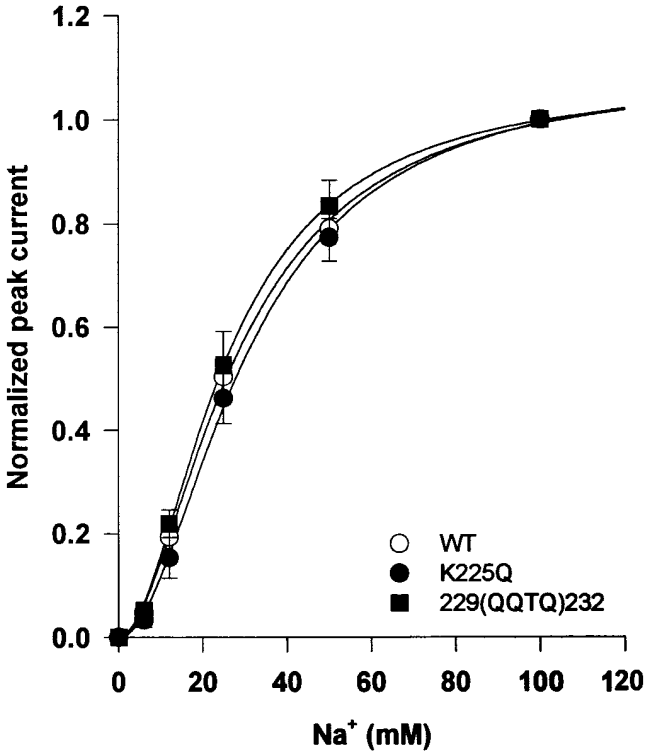

FIGURE 4. Na^+ dependence of the Na^+-Ca^{2+} exchanger transport cycle. Currents were normalized at the peak current for the wild type and group 1 mutants and normalized at 2 s after Na^+ application for the group 2 mutants. Data (mean ± SD) of the wild type (*open circles*), a representative group 1 mutant (K225Q, *filled circles*) and a representative group 2 mutant (229(QQTQ)232, *filled squares*) are shown as examples. Curves are fits to the Hill equation.

TABLE IV

Apparent Na^+ Affinities

	$K_h(Na^+)$ ± SD (in mM)		
Mutant	I_{peak}	Fss	Iss
Wild-type	28 ± 1 (4)	8 ± 1 (4)	—
F223E	28 ± 5 (4)	6 ± 1 (5)	—
Y224T	24 ± 4 (3)	9 ± 2 (3)	—
K225Q	31 ± 4 (4)	13 ± 1 (4)	—
Y226T	26 ± 4 (4)	8 ± 2 (4)	—
K229Q	33 ± 6 (5)	—	35 ± 9 (4)
R230Q	30 ± 4 (4)	12 ± 5 (4)	—
Δ229–232	29 ± 1 (4)	—	33 ± 4 (4)
229(QQTQ)232	26 ± 3 (4)	—	25 ± 1* (4)
Δ229–237	29 ± 4 (4)	—	30 ± 4 (4)

The apparent Na^+ affinities for peak current (I_{peak}), fractional steady-state current (Fss), and steady-state current (Iss) were determined. See Figs. 4, 5, and 6 for details. Values for *n* are given in parentheses. Mutants belonging to group 2 are shaded. *$P < 0.01$ compared to I_{peak} of wild-type.

sumed that the inactivated state arises from exchangers with three Na^+ bound at the intracellular surface though possibly some Na^+-dependent inactivation occurs from partially Na^+-loaded exchangers.

In Fig. 5 *B*, Fss values of group 2 mutants are plotted against Na^+ concentration. Fss values were close to 1.0 at all Na^+ concentrations examined, indicating no obvious current inactivation during Na^+ application.

Group 2 Mutants: No Inactivation or Undetectable Inactivation?

As seen above, no clear current decay was observed in group 2 mutant Na^+-Ca^{2+} exchangers under our experimental conditions. A simple interpretation is that there is no Na^+-dependent inactivation in group 2 mutants. However, an alternative possibility is that the inactivation occurred too rapidly to be detected by our technique. This possibility was examined in the following experiments.

Na^+-dependent inactivation alters the Na^+ dependency of the wild-type Na^+-Ca^{2+} exchange current (Fig. 6 *A*). Na^+ dependencies were measured at both the initial peak and at steady state, after inactivation had occurred. Both the peak and steady-state currents were normalized to currents at 100 mM Na^+, and the normalized currents plotted as a function of Na^+ concentration. The peak current saturates at about 100 mM Na^+ and the curve can be fit to the Hill equation with a $K_h(Na^+)$ of 28 mM, a Hill coefficient of 1.8, and a maximum current of 1.1.

The wild-type steady-state current, however, does not begin to saturate even at 100 mM, and the curve cannot be reasonably fit to the Hill equation (a $K_h(Na^+)$ = 1,197 mM, $n = 0.8$, and current maximum = 7.5 is obtained when attempting a fit). The lack of fit of the wild-type exchanger steady state current to the Hill equation is probably a consequence of the increase in Fss seen for the wild-type and group 1 exchangers at 100 mM Na^+ (Fig. 5 *A*). The reason for the smaller than expected inactivation at high Na^+ (Fig. 5 *A*) is unexplained and demonstrates the complexity of the inactivation process. Nevertheless, the effect results in an increased exchange current and a failure to saturate.

The Na^+ dependencies of the steady state currents of group 2 mutants are shown in Fig. 6 *B*. Like the wild-type peak current, the mutant steady-state currents saturate at about 100 mM Na^+ and the curves can be fit using the Hill equation. The calculated $K_h(Na^+)$ values for the wild-type peak current and the group 2 steady-state currents is shown in Table IV, data columns 1 and 3. The $K_h(Na^+)$ for each of the group 2 mutants is very close to that of the wild-type peak current. If the group 2 mutants possessed a Na^+-dependent inactive state, it would be predicted that the $K_h(Na^+)$ for the steady-state current would be high as seen for the wild-type and group 1 exchangers. Therefore, these data suggest that

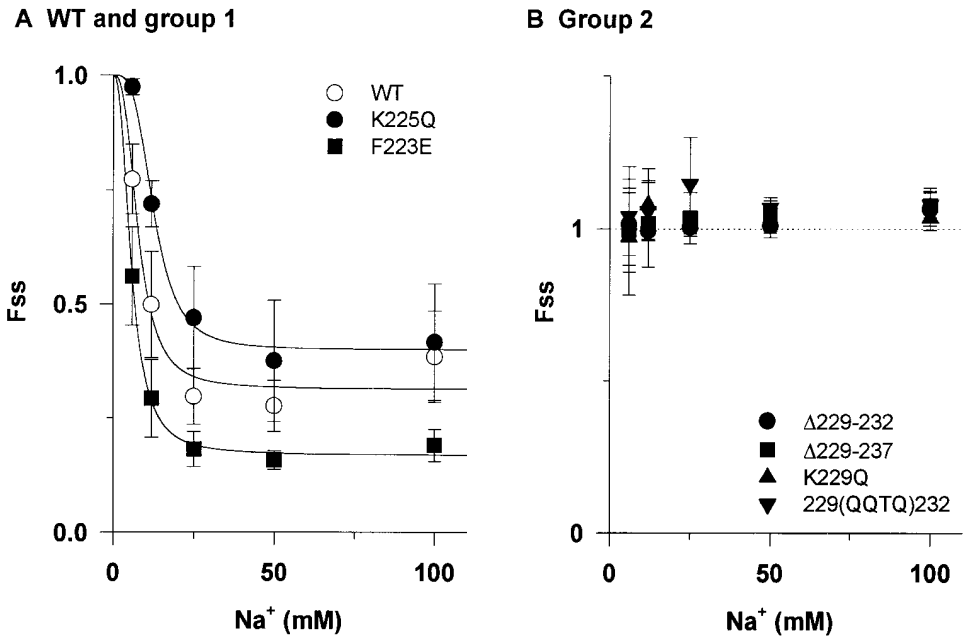

FIGURE 5. Na^+ dependence of the Na^+-dependent inactivation. (*A*) Na^+ concentration-Fss relation for group 1 mutants. Fss values, the ratio of steady-state to peak currents, are plotted versus different Na^+ concentrations. See text for detail. (*B*) Fss values of group 2 mutants. Fss values of group 2 mutants are plotted against different Na^+ concentrations. It is notable that Fss is close to 1.0 at all Na^+ concentrations studied.

the Na^+-dependent inactive state does not exist in mutants K229Q, Δ229–232, 229(QQTQ)232, and Δ229–237.

To further examine the possibility of Na^+-dependent inactivation in group 2 mutants, the inward exchanger currents were examined for the wild-type exchanger and one group 2 mutant, K229Q (Fig. 7). With 140 mM Na^+ and 2 mM Ca^{2+} in the pipette (extracellular) solution, either the outward or inward Na^+-Ca^{2+} exchange current can be recorded by including 100 mM Na^+, 1 μM Ca^{2+} (for outward currents) or 0 mM Na^+, 1 μM Ca^{2+} (for inward currents) in the cytoplasmic solution.

For the wild-type exchanger (Fig. 7 *A*), a cytoplasmic solution containing no Na^+ and no Ca^{2+} was preapplied. Under this condition the exchanger does not function. A solution switch to 0 mM Na^+, 1 μM Ca^{2+} induced the inward Na^+-Ca^{2+} exchange current. This was followed by a switch to a solution containing 100 mM Na^+, 1 μM Ca^{2+} to activate the outward exchange current. The peak outward current was about twofold larger than the inward Na^+-Ca^{2+} exchange current. The outward exchange current decayed in a time-dependent manner. The magnitude of the outward current at steady-state was somewhat less than the magnitude of the steady-state inward current. Removing the cytoplasmic Na^+ reactivated the inward Na^+-Ca^{2+} exchange current. However, the rate of activation of the inward

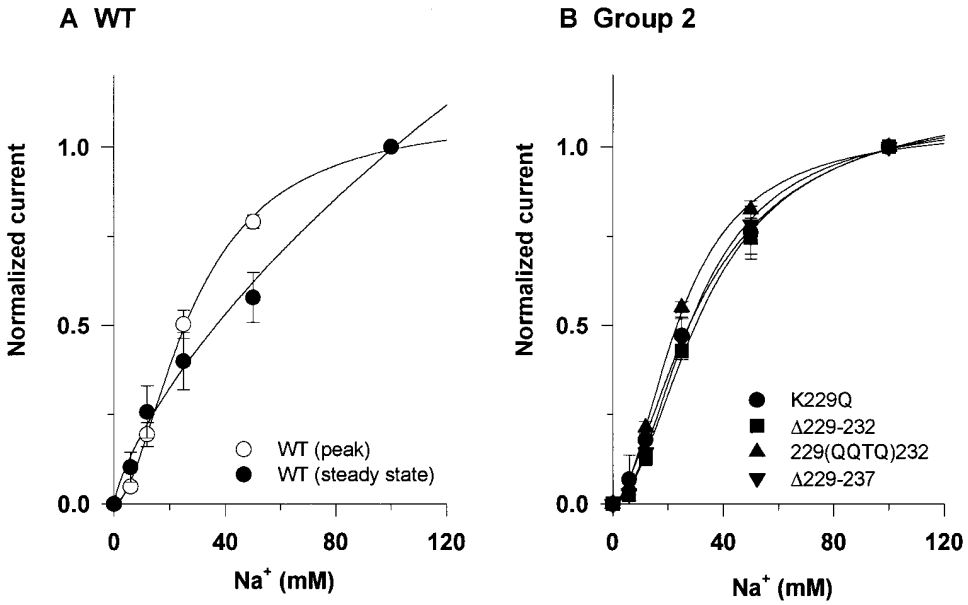

FIGURE 6. Na^+-dependence of wild-type and group 2 mutants. (*A*) Peak and steady-state Na^+ dependence of the wild-type Na^+-Ca^{2+} exchanger. Normalized peak (*open circles*) and steady-state (*filled circles*) currents are plotted as a function of cytoplasmic Na^+. Curves are fits to the Hill equation. See text for details. (*B*) Steady-state Na^+ dependence of group 2 mutants. Normalized steady state currents are plotted in a similar manner as for the wild-type exchanger.

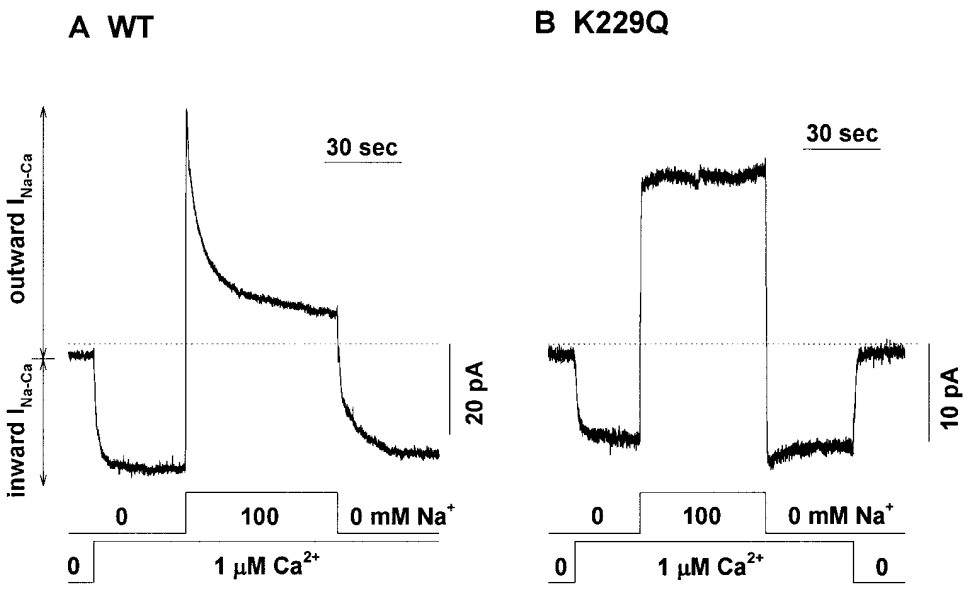

FIGURE 7. Recording of outward and inward Na^+-Ca^{2+} exchange currents in excised patches from oocytes expressing wild-type and K229Q Na^+-Ca^{2+} exchangers. The pipette solution contained both Na^+ (140 mM) and Ca^{2+} (2 mM). Cytoplasmic Na^+ and Ca^{2+} concentrations are noted under the current traces. (*A*) Recording of outward (application of Na^+) and inward (application of Ca^{2+} in the absence of Na^+) currents from the wild-type exchanger. (*B*) Recordings of outward and inward currents from mutant exchanger K229Q. Note the amplitude ratio of the outward to the inward currents. Also, for the two exchangers compare the time courses of activation of the inward current by (*a*) addition of intracellular Ca^{2+} and (*b*) removal of intracellular Na^+.

current was slower when induced by the removal of Na^+ than when induced by the addition of Ca^{2+}. This slow activation reflects recovery from the Na^+-dependent inactive state. Essentially the same results were obtained in five oocytes.

Fig. 7 *B* represents the Na^+-Ca^{2+} exchange current from a group 2 mutant, K229Q. The current induction protocol was identical to that just described for the wild-type exchanger. The outward current amplitude was also about twofold larger than the inward current, but the current did not decay during Na^+ application. The activation of the inward current by removing 100 mM Na^+ was instantaneous and did not show recovery from inactivation. Similar results were obtained in six oocytes. As discussed below, these results demonstrate that the Na^+-dependent inactivation process does not exist in K229Q. Essentially the same results were obtained with mutants 229(QQTQ)232 (n = 1) and Δ229–232 (n = 2).

Effects of Intracellular Ca^{2+} on XIP Region Mutants

In addition to being transported, Ca^{2+} also plays a role in regulating the exchanger. Ca^{2+} binds to a high affinity, nontransport site at the intracellular surface of the exchanger. When this regulatory Ca^{2+} is removed, the exchanger enters I_2, a Na^+-independent inactivated state. Return of Ca^{2+} to the cytoplasmic face restores exchange activity. Ca^{2+} also modulates the Na^+-dependent inactivated state of the exchanger (I_1). Increases of intracellular Ca^{2+} accelerate the rate of recovery from I_1 (Hilgemann et al., 1992*a*, *b*; Matsuoka et al., 1995). These effects of intracellular Ca^{2+} on I_1 and I_2 can be seen in Fig. 8. In the wild-type exchanger, application of intracellular Na^+ (*crosshatched bar*), in the presence of increasing concentrations of cytoplasmic Ca^{2+} (0–10 μM), enhances the peak current and suppresses Na^+-dependent inactivation. The peak current stimulation is saturable; at 10 μM Ca^{2+}, the peak current was only 20% larger than the current at 0.5 μM. Also, the inactivation was almost completely abolished in 10 μM Ca^{2+}. Augmentation of the peak current by cytoplasmic Ca^{2+} has previously been attributed to recovery from I_2 (Na^+-independent inactivation; Hilgemann et al., 1992*a*) while the increase in Fss implies suppression of I_1 by Ca^{2+}.

The effects of intracellular Ca^{2+} on exchange activity of the XIP region mutants were also examined. As with the wild-type exchanger, increasing regulatory Ca^{2+} stimulated the outward exchange currents of all XIP region mutants (Fig. 8). However, in group 1 mutants, the peak current at 10 μM Ca^{2+} was about 1.5 to 3 times larger than the current at 0.5 μM Ca^{2+}, implying a possible decrease in apparent Ca^{2+} affinity. At low Ca^{2+} concentration, group 2 mutants display a slow current increase upon applying 100 mM Na^+ (Fig. 8). The mechanism for the slow activation is not understood at present.

The apparent Ca^{2+} affinity was investigated as shown in Fig. 9. The peak of the outward current upon application of Na^+ is measured before significant Na^+-dependent inactivation occurs. Therefore, the dependence of the peak exchanger current on Ca^{2+} concentration is a measure of the apparent affinity of the exchanger for regulatory Ca^{2+}. We determined the dependencies of

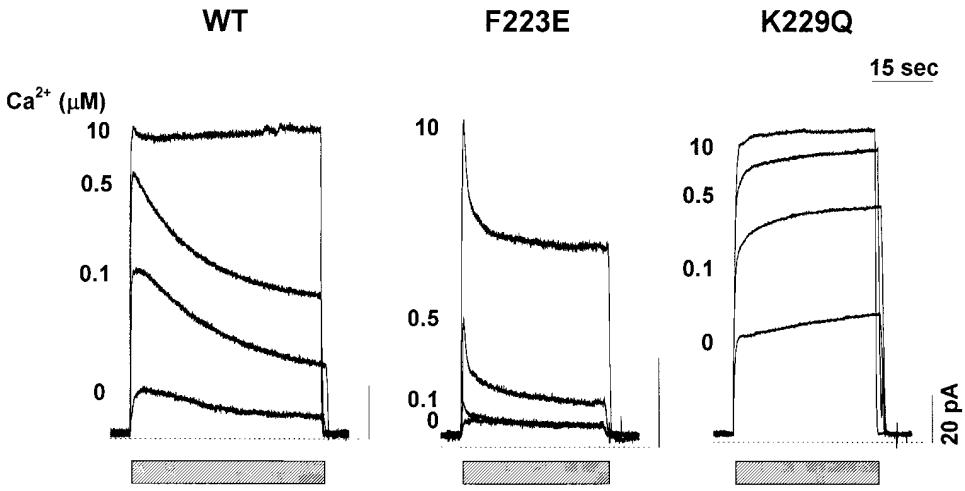

FIGURE 8. Effect of intracellular Ca^{2+} on activation of the outward Na^+-Ca^{2+} exchange current in the wild-type (*WT*), F223E (a group 1 mutant), and K229Q (a group 2 mutant) exchangers. The currents were induced by applying 100 mM cytoplasmic Na^+ in the presence of 0, 0.1, 0.5, 1, and 10 μM cytoplasmic Ca^{2+}.

the exchange currents on regulatory Ca^{2+} concentration (Fig. 9). For group 1 and wild-type exchange currents, the peak currents were measured. For group 2 mutants, steady-state currents, which are essentially the same as peak currents (Table I, Fig. 1), were measured. For all exchangers, the current declines at more than 10 μM Ca^{2+}. The current decline is due to competition between Ca^{2+} and Na^+ at the ion transport site. Therefore the declining phases were omitted for fitting to the Hill equation.

The Ca^{2+} concentration–peak current relationships for all group 1 mutants are shifted to higher Ca^{2+} concentrations relative to the wild-type exchanger. $K_h(Ca^{2+})$ values for peak currents are 3–6 times higher in group 1 mutants than for the wild-type exchanger (Table V, 1st data column). These data indicate that some mutations in the XIP region of the exchanger reduce the apparent affinity of the exchanger for regulatory Ca^{2+}.

The Ca^{2+} concentration–steady-state current relationships for the group 2 mutants are almost superimposable with those for the wild-type exchanger, though Δ229–237 displays a large Ca^{2+}-insensitive component (not shown). The $K_h(Ca^{2+})$ values for group 2 mutants remain essentially unchanged from the wild-type exchanger. Therefore, the group 1 mutations affect regulatory Ca^{2+} affinity, but the group 2 mutations have no effect on the apparent affinity.

In the wild-type Na^+-Ca^{2+} exchanger, the apparent affinity for regulatory Ca^{2+} is lower at steady-state than at peak current. This apparent change in affinity was modelled to be due to an affect of Ca^{2+} on Na^+-dependent inactivation (I_1) (Hilgemann et al., 1992*b*). To determine if Ca^{2+} regulation of I_1 is altered in group 1 mutants, the quasi-steady state Ca^{2+} dependencies of wild type and group 1 mutant exchangers were determined (Fig. 10, *A* and *B*; Table V). For two of the mutants, R230Q and Y226T, the Ca^{2+} concentration–steady-state current relationships are almost superimposable with wild type (Fig. 10 *A*). However, for the remaining group 1 mutants, F223E, Y224T, and K225Q, the relationships are shifted towards higher Ca^{2+} concentrations (Fig 10 *B*, Table V, 2nd data column). Thus, the apparent affinity for regulatory Ca^{2+} in Na^+-dependent inactivation of group 1 mutants F223E, Y224T, and K225Q is reduced.

In Fig. 8, it also appeared that for the group 1 mutants Na^+-dependent inactivation was less suppressed than for the wild-type exchanger. Therefore, the effect of intracellular Ca^{2+} on the Fss of group 1 mutants was

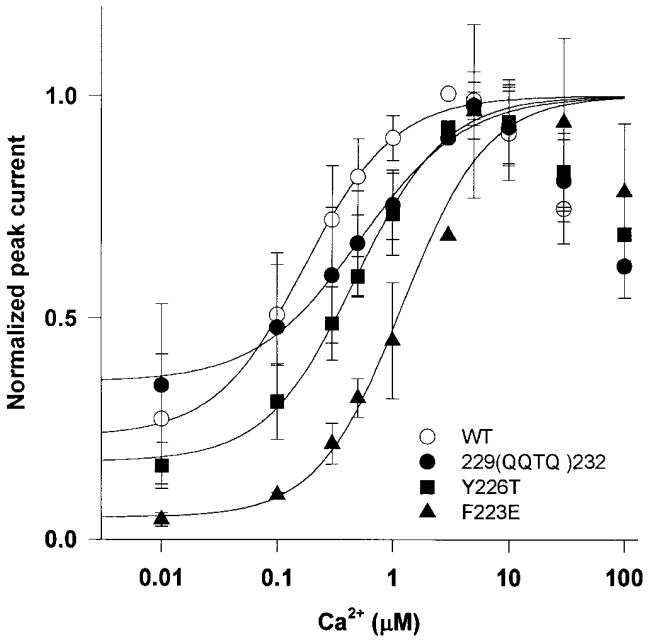

FIGURE 9. Cytoplasmic Ca^{2+} dependence of peak currents from wild-type (*WT*) and group 1 (*Y226T, F223E*) exchangers and steady-state currents from a group 2 (*229(QQTQ)232*) exchanger. Steady-state currents were measured ~40 s after 100 mM Na^+ application. The curves were normalized to the fitted maximal current.

TABLE V

Cytoplasmic Ca^{2+} Dependencies

Mutant	$K_h(Ca^{2+})$ ± SD (μM)		
	Peak	Steady State	Fss
Wild-type	0.2 ± 0.2 (6)	0.8 ± 0.4 (6)	2.3 ± 2.1 (6)
F223E	1.2 ± 0.1‡ (3)	5.5 ± 1.3‡ (3)	16.8 ± 2.0‡ (3)
Y224T	0.8 ± 0.2‡ (3)	2.6 ± 1.0‡ (3)	8.7 ± 4.4* (3)
K225Q	0.8 ± 0.2‡ (4)	2.5 ± 0.9‡ (4)	6.8 ± 1.2‡ (4)
Y226T	0.7 ± 0.4* (3)	1.2 ± 0.3 (3)	3.9 ± 1.4 (3)
R230Q	0.6 ± 0.5 (3)	0.9 ± 0.1 (3)	1.2 ± 0.4 (2)
K229Q	0.2 ± 0.1 (4)		
Δ229–232	0.2 ± 0.1 (5)		
229(QQTQ)232	0.5 ± 0.3 (4)		
Δ229–237	0.3 ± 0.2 (3)		

The cytoplasmic Ca^{2+} dependencies of Fss and peak and steady-state outward exchange currents in XIP region mutants were determined. Values for *n* are given in parentheses. Mutants belonging to group 2 are shaded. $^*P < 0.05$, $^‡P < 0.01$

examined (Fig. 10 *C*, Table V). In R230Q and Y226T, the relationship was nearly superimposable with wild type (not shown) and the $K_h(Ca^{2+})$ (the concentration of Ca^{2+} at which relief from Na^+-dependent inactivation was half maximal) was unaltered (Table V, 3rd data column). In Y224T and K225Q (not shown), the relationship shifted to higher Ca^{2+} concentrations and there was about a threefold increase in $K_h(Ca^{2+})$ (Table V, 3rd data column). In F223E, the relationship shifted even further. Thus, in mutants F223E, Y224T, and K225Q, Na^+-dependent inactivation is less sensitive to intracellular Ca^{2+}.

Responses to Ca^{2+} Removal and Application

As just described, Ca^{2+} regulation of Na^+-dependent inactivation was altered in the group 1 mutants. Ca^{2+} regulation in the XIP region mutants was further examined by measuring the rate of change of current in response to removing and applying intracellular Ca^{2+}. Fig. 11 illustrates outward Na^+-Ca^{2+} exchange current responses to removing and reapplying Ca^{2+} in the wild-type exchanger and in group 1 (F223E, Y224T) and group 2 (229(QQTQ)232) mutants. Ca^{2+} (1 μM) was removed and reapplied in the presence of 100 mM Na^+. For the wild-type exchanger, the current change upon removing and applying Ca^{2+} is very slow. The current change consists of rapid and slow components, which may correspond to entry of the exchanger into the active or inactive states via effects on both Na^+-dependent (I_1) and Na^+-independent (I_2) processes (Hilgemann et al., 1992*a*). For F223E and Y224T, and all other group 1 mutants, the response to Ca^{2+} removal and application was much more rapid than in wild type. Similarly, 229(QQTQ)232 and all other group 2 mutants

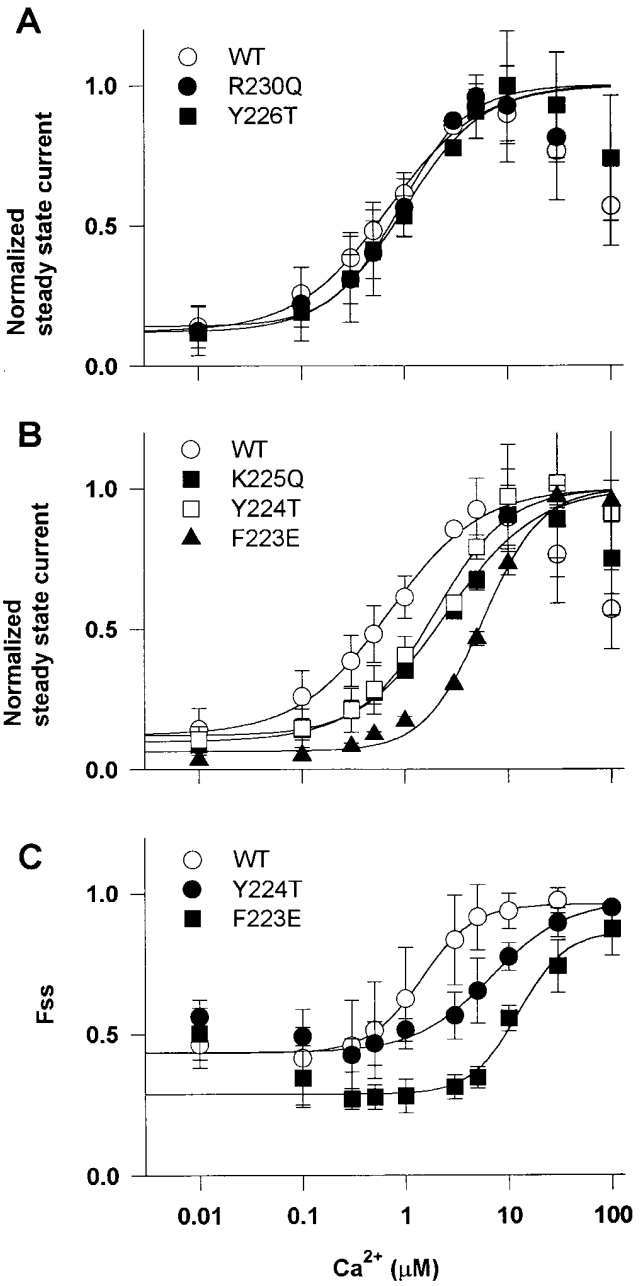

FIGURE 10. Cytoplasmic Ca^{2+} dependence of steady state currents from group 1 mutants (*A* and *B*). Curves are fits to the Hill equation. (*C*) Inhibition of Na^+-dependent inactivation by intracellular Ca^{2+}. Fss values are plotted against the Ca^{2+} concentration. The data at 0.01 μM Ca^{2+} (*WT*, *Y224T*, and *F223E*) and at 0.1 μM Ca^{2+} (*F223E*) were omitted for fitting to the Hill equation.

exhibited rapid responses to Ca^{2+} concentration changes.

Table VI summarizes the half-time (t_h) for the exchanger to reach steady-state current after the change in intracellular Ca^{2+}. In all XIP region mutants, t_h values were significantly less than for the wild type. This tendency was especially notable in the group 2 mutants.

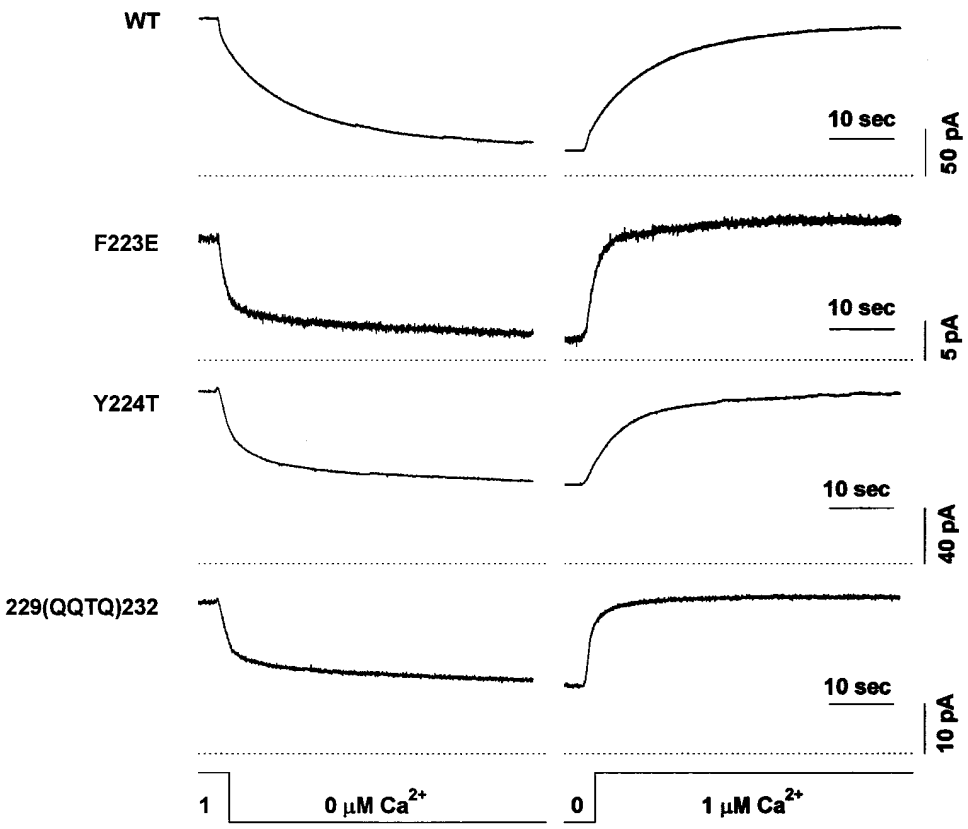

FIGURE 11. Responses of outward Na^+-Ca^{2+} exchange currents in wild type (*WT*) and mutant exchangers to removal and reapplication of 1 μM intracellular Ca^{2+}. 100 mM Na^+ was present in all cytoplasmic solutions.

DISCUSSION

Mutations in the Endogenous XIP Region of the Na^+-Ca^{2+} Exchanger Affect Regulation

XIP is a 20 amino acid peptide with a sequence corresponding to the amino-terminal end of the large intracellular loop of the Na^+-Ca^{2+} exchanger. When exogenous XIP peptide is applied to the intracellular surface, the exchanger is inhibited (Li et al., 1991). We therefore proposed that the XIP region of the exchanger, by analogy to the effects of exogenous XIP, also interacts with a XIP-binding site to modulate activity. To gain insight into the role of the exchanger XIP region, we have introduced mutations in the XIP region and examined the properties of the mutants. The results indicate that the endogenous XIP region is indeed involved in regulatory aspects of exchanger function.

We constructed nine Na^+-Ca^{2+} exchangers with mutations in the XIP region. The phenotypes of these mutants all fall into two categories designated group 1 or group 2. Two regulatory properties are affected in the mutants: Na^+-dependent inactivation and Ca^{2+} regulation. XIP-region mutants have both altered Na^+-dependent inactivation and Ca^{2+} regulation though the effects on inactivation are more striking.

In group 1 mutants, Na^+-dependent inactivation is still displayed but the kinetics of inactivation are altered. In group 2 mutants, the Na^+-dependent inactivation process is completely absent. The altered kinetics in the group 1 mutants are seen as an increase in the rate of the inactivation process (Table II). In one case, F223E, the $T_{1/e}$ decreases over sixfold. Inactivation in the wild-type exchanger is quite slow with a $T_{1/e}$ of almost 9 s. Presumably, slow conformational changes of the exchanger protein are occurring during this time. Apparently, the conformational changes occur more rapidly in the group 1 mutants. Thus, steady state is achieved more quickly.

In contrast, the four group 2 XIP region mutants do not display any Na^+-dependent inactivation. Inactivation is not detectable in current traces (Fig. 1), and Fss is about 1 for all group 2 mutants (Table I). There are two possibilities to explain these observations. Either inactivation occurs too rapidly to be observed by our techniques or inactivation no longer occurs. Three observations strongly support the latter possibility.

First, the apparent affinity for Na^+ of the wild-type exchanger is different before and after inactivation. The apparent Na^+ affinity for the initial peak, before inactivation, is much higher than that during steady state, after inactivation (Fig. 6 *A*). If inactivation had occurred for the group 2 mutants, then the Na^+ affinity should resemble that of the wild-type exchanger during steady-state measurements. However, the apparent Na^+ affinity of the group 2 mutants at steady state is similar to that of the wild-type exchanger at initial peak current

TABLE VI

Half-time to Reach Steady State

Mutant	t_h (s) ± SD (n)	
	Ca^{2+} off	Ca^{2+} on
Wild-type	10.5 ± 5.8 (9)	9.6 ± 3.3 (9)
F223E	3.3 ± 2.2* (4)	2.5 ± 1.1‡ (5)
Y224T	4.2 ± 1.5* (6)	4.8 ± 0.5‡ (6)
K225Q	4.2 ± 1.3* (6)	4.1 ± 1.0‡ (7)
Y226T	3.7 ± 0.9* (4)	3.5 ± 0.6‡ (4)
K229Q	1.0 ± 0.2‡ (4)	1.0 ± 0.3‡ (4)
R230Q	2.6 ± 0.8‡ (7)	2.6 ± 0.9‡ (7)
Δ229–232	0.9 ± 0.5‡ (6)	0.8 ± 0.4‡ (7)
229(QQTQ)232	2.1 ± 1.4‡ (6)	1.7 ± 0.9‡ (7)
Δ229–237	0.6 ± 0.5‡ (11)	0.5 ± 0.4‡ (9)

The half-time to reach steady-state level of outward exchange current upon removing (Ca^{2+} off) and adding (Ca^{2+} on) 1 μM of Ca^{2+} is shown. *$P < 0.05$, ‡$P < 0.01$.

values before inactivation (Fig 6 *B*) and does not display the altered relationship expected from an exchanger with Na^+-dependent inactivation.

Second, for the wild-type exchanger the existence of Na^+-dependent inactivation results in a decrease in the apparent affinity for regulatory Ca^{2+} in the steady state current compared to the peak current (Table V, data columns 2 and 3). The group 2 mutants display affinities for regulatory Ca^{2+} which are nearly the same as for the wild-type peak current, lending further support for absence of Na^+-dependent inactivation of the group 2 mutants.

Third, the comparison of inward versus outward exchange currents (Fig. 7) also demonstrates the absence of inactivation in group 2 mutants. For the study in Fig. 7, the pipette solution contained both Na^+ and Ca^{2+} allowing either inward or outward currents to be measured in the same excised patch by manipulating the bath solution. For the wild-type Na^+-Ca^{2+} exchanger, the amplitude of the peak outward exchange current is substantially larger than that of the inward exchange current. After the inactivation process, the amplitude of the steady-state outward current is close to that of the inward current. For group 2 mutants under identical conditions, the outward current amplitude is larger than that of the inward current, analogous to the wild-type exchanger current before inactivation. Furthermore, slow recovery from Na^+-dependent inactivation was not observed, and the activation of inward current by removing Na^+ was instantaneous. These observations provide strong evidence that no inactivation occurs for the group 2 mutants.

Apparently, the mutations introduced into the group 2 exchangers prevent the conformational changes and interactions which allow the inactivation process to occur. The implication is that the XIP region of the Na^+-Ca^{2+} exchanger is directly involved in the inactivation process. The XIP region is modeled to be near the membrane interface and conformational changes in this critical area could easily modulate ion transport. Alternatively, the XIP region mutations could be perturbing distantly located regions of the exchanger protein to alter inactivation. The fact that single-site mutations (e.g., K229Q or R230Q) have major effects on inactivation perhaps argues against this possibility. Strikingly, all nine mutants in the XIP region had altered inactivation, demonstrating the sensitivity of inactivation to modification of this region.

The Na^+ Affinities for Transport Cycle and Regulation Are Unaffected by XIP Region Mutations

The apparent affinities of the wild type and mutant exchangers for Na^+, as calculated from the relationship between peak current and Na^+ concentration, are essentially identical (Fig. 4; Table IV, data columns 1 and 3), indicating that the Na^+ affinity for the transport cycle is unaffected by mutation in the XIP region.

The extent of Na^+-dependent inactivation of the Na^+-Ca^{2+} exchanger also varies with Na^+ concentration (Fig. 5 *A*). Fss, a measure of Na^+-dependent inactivation, decreases as Na^+ increases, indicating increased inactivation. The Na^+ dependence of Fss is virtually identical for the wild-type and group 1 mutant exchangers (Fig. 5 *A*; Table IV, data column 2), indicating that the apparent affinity for Na^+-dependent regulation is also unaffected by XIP region mutations.

These data are consistent with a model for exchanger entry into the I_1 inactive state from the fully sodium-loaded conformation (Hilgemann et al., 1992*b*). Both transport and entry into I_1 are modelled to be dependent upon Na^+ binding to the transport sites. The fact that the Na^+ dependencies of both transport and inactivation are unaffected by the mutations indicates that the effects of the mutations on inactivation occurs subsequent to the ion binding event.

The Ca^{2+} Affinity of Regulation Is Altered in Group 1 Mutants

An indication that the affinity of regulatory Ca^{2+} is altered in the group 1 XIP region mutants can be seen in Fig. 8. The exchanger peak activities are stimulated by increasing levels of regulatory Ca^{2+}. At 10 μM Ca^{2+}, the peak current of the wild-type exchanger is nearly saturated, but the peak currents of the group 1 mutants are not. The $K_h(Ca^{2+})$ for stimulation of exchanger peak currents by regulatory Ca^{2+} was determined to be 3-6 times higher than for the wild-type exchanger (Table V, data column 1).

Cytoplasmic Ca^{2+} directly modulates exchange activity but also modulates the Na^+-dependent inactivation

process (Hilgemann, 1990; Hilgemann et al., 1992*b*). As regulatory Ca^{2+} increases, inactivation is suppressed and higher steady state currents result (Fig. 8). The group 1 XIP region mutants show a reduced suppression of Na^+-dependent inactivation by Ca^{2+} relative to the wild-type exchanger (Fig. 8). At 10 μM Ca^{2+}, the inactivation is nearly completely suppressed in wild type whereas group 1 mutants still display significant levels of inactivation. The dependence of F223E, Y224T, and K225Q steady-state currents on regulatory Ca^{2+} is shifted toward higher Ca^{2+} concentration (Fig. 10 *B*) than for the wild-type exchanger and the $K_h(Ca^{2+})$ is significantly higher for these mutants (Table V, data column 2).

Thus, the group 1 mutations have decreased apparent Ca^{2+} affinities for two separate functions: the ability to activate peak exchange current and to suppress Na^+-dependent inactivation. The fact that both apparent Ca^{2+} affinities are affected in a similar manner is consistent with the proposal that both modulatory functions are due to the binding of Ca^{2+} to the same Ca^{2+} regulatory site.

Surprisingly, group 2 mutants do not appear to have altered regulatory Ca^{2+} affinity (Table VI). This is in spite of the fact that one of the mutated residues in a group 2 mutant, K229, is sandwiched between two group 1 mutants, Y226T and R230Q. Also the remaining group 2 mutants (Δ229–232, 229(QQTQ)232, and Δ229–237) include mutation at residue R230 whereas the point mutant R230Q belongs in group 1.

Both group 1 and 2 mutants, however, respond much more quickly than the wild-type exchanger to changes in regulatory Ca^{2+} (Fig. 11, Table VI). The wild-type Na^+-Ca^{2+} exchanger responds slowly (t_h is ~10 s) to changes in regulatory Ca^{2+}. Presumably, the actual Ca^{2+}-binding event is rapid and the slow response to regulatory Ca^{2+} is due to subsequent conformational changes. As previously modeled (Hilgemann et al., 1992*b*), these kinetics are partly dependent on the rate of Na^+-dependent inactivation. When Na^+-dependent inactivation is accelerated (group 1 mutants) or absent (group 2 mutants), responses to changes in regulatory Ca^{2+} are also accelerated as the appropriate conformational changes apparently can occur more rapidly. Similar conformational changes may be responsible for the slowness of both the Na^+-dependent inactivation and secondary Ca^{2+} regulation of the wild-type Na^+-Ca^{2+} exchanger.

Na^+-dependent inactivation and Ca^{2+} regulation are clearly interacting processes. It has previously been reported that Ca^{2+} affects inactivation. First, Ca^{2+} modulates the extent of Na^+-dependent inactivation (Hilgemann et al., 1992*b*). Second, mutations which affect Ca^{2+} binding also affect inactivation (Matsuoka et al., 1995). Here, we demonstrate the converse: mutations which primarily affect Na^+-dependent inactivation also affect Ca^{2+} regulation.

Concluding Comments

We had proposed that the XIP region of the Na^+-Ca^{2+} exchanger had an autoregulatory function (Li et al., 1991). Mutational analysis of the XIP region provides strong supportive evidence for such a role. Single-site mutations modulate or abolish Na^+-dependent inactivation of the Na^+-Ca^{2+} exchanger. In this study, we focussed on mutation of the basic and aromatic residues of the XIP region. These residues are shown in a separate study (He et al., 1997) to be important for the inhibitory action of exogenously added XIP peptides and are shown here to be important for autoregulation.

The precise molecular basis for Na^+-dependent inactivation and the role of the XIP region are unknown. One possible mechanism for the regulation of the exchanger by cytoplasmic Na^+ and Ca^{2+} is as follows: Upon application of Na^+ to the cytoplasmic face, the exchanger translocates Na^+ and Ca^{2+} across the membrane. At the same time, the XIP-region slowly binds to a docking site on the protein. The docking of XIP is observed as Na^+-dependent inactivation (I_1) of the exchange current. Regulatory Ca^{2+} binds to the Ca^{2+}-binding site of the intracellular loop and produces a conformational change of the exchanger. This Ca^{2+}-induced conformational change hampers XIP docking, and increases peak and steady state outward current.

The physiological role of Na^+-dependent inactivation is also unknown but the presence of active and inactive states may provide flexibility for regulation of the Na^+-Ca^{2+} exchanger by various modulatory influences. For example, the cardiac exchanger is modulated by intracellular ATP levels (Hilgemann et al., 1992*a*; Condrescu et al., 1995) through PIP_2-dependent (Hilgemann and Ball, 1996), and protein kinase C dependent (Iwamoto et al., 1996) mechanisms. These modulations of the exchanger may act by altering the inactivation process. Under physiologic conditions, the myocyte intracellular Na^+ concentration is about 10 mM. At this concentration, about half of the exchangers may be in the I_1-inactive state (Table IV). Changes in cytoplasmic factors (e.g., Ca^{2+} or ATP) under physiologic or pathologic conditions may alter the distribution between active and inactive states.

We appreciate Dr. A. Noma for his helpful discussions, and we thank Mr. Hang, Dr. L. Lu, Dr. Kohno, and Dr. Ishii for their technical assistance. We also thank Dr. J. Weiss for commenting on the manuscript.

This work was supported by National Institutes of Health grants HL48509 and HL49101, the Laubisch Foundation, and by a grant from the American Heart Association, Greater Los Angeles Affiliate to D.A. Nicoll and a Grant-in-Aid for Scientific Research from the Ministry of Education, Science and Culture to S. Matsuoka.

Original version received 16 September 1996 and revised version received 18 November 1996.

REFERENCES

Bers, D.M., C.W. Patton, and R. Nuccitelli. 1993. A practical guide to the preparation of Ca^{2+} buffers. *Methods Cell Biol.* 40:3–29.

Condrescu, M., J.P. Gardner, G. Chernaya, J.F. Aceto, C. Kroupis, and J.P. Reeves. 1995. ATP-dependent regulation of sodium-calcium exchange in chinese hamster ovary cells transfected with the bovine cardiac sodium-calcium exchanger. *J. Biol. Chem.* 270: 9137–9146.

DiPolo, R. 1979. Calcium influx in internally dialyzed squid giant axons. *J. Gen. Physiol.* 73:91–113.

He, Z., N. Petesch, K.-P. Voges, W. Roben, and K.D. Philipson. 1997. Identification of important amino acid residues of the Na^+-Ca^{2+} exchanger inhibitory peptide, XIP. *J. Membr. Biol.* In press.

Hilgemann, D.W. 1989. Giant excised cardiac sarcolemmal membrane patches: sodium and sodium-calcium exchange currents. *Pflüg. Archiv.* 415:247–249.

Hilgemann, D.W. 1990. Regulation and deregulation of cardiac Na^+-Ca^{2+} exchange in giant excised sarcolemmal membrane patches. *Nature (Lond.).* 344:242–245.

Hilgemann, D.W., and R. Ball. 1996. Regulation of cardiac Na^+,Ca^{2+} exchange and K_{ATP} potassium channels by PIP_2. *Science (Wash. DC)*. 273:956–959.

Hilgemann, D.W., A. Collins, and S. Matsuoka. 1992*a*. Steady state and dynamic properties of cardiac sodium-calcium exchange: secondary modulation by cytoplasmic calcium and ATP. *J. Gen. Physiol.* 100:933–961.

Hilgemann, D.W., S. Matsuoka, G.A. Nagel, and A. Collins. 1992*b*. Steady state and dynamic properties of cardiac sodium-calcium exchange: sodium-dependent inactivation. *J. Gen. Physiol.* 100: 905–932.

Hilgemann, D.W., D.A. Nicoll, and K.D. Philipson. 1991. Charge movement during Na^+ translocation by native and cloned cardiac Na^+/Ca^{2+} exchangers. *Nature (Lond.).* 352:715–718.

Iwamoto, T., Y. Pan, S. Wakabayashi, T. Imagawa, H.I. Yamanaka, and M. Shigekawa. 1996. Phosphorylation-dependent regulation of cardiac Na^+/Ca^{2+} exchanger via protein kinase C. *J. Biol. Chem.* 271:13609–13615.

Levitsky, D.O., D.A Nicoll, and K.D. Philipson. 1994. Identification of the high affinity Ca^{2+}-binding domain of the cardiac Na^+-Ca^{2+} exchanger. *J. Biol. Chem.* 269:22847–22852.

Li, Z., D.A. Nicoll, A. Collins, D.W. Hilgemann, A.G. Filoteo, J.T. Penniston, J.N. Weiss, J.M. Tomich, and K.D. Philipson. 1991. Identification of a peptide inhibitor of the cardiac sarcolemmal Na^+-Ca^{2+} exchanger. *J. Biol. Chem.* 266:1014–1020.

Longoni, S., M.J. Coady, T. Ikeda, and K.D. Philipson. 1988. Expression of cardiac sarcolemmal Na^+-Ca^{2+} exchange activity in *Xenopus laevis* oocytes. *Am. J. Physiol.* 255:C870–C873.

Matsuoka, S., and D.W. Hilgemann. 1992. Steady-state and dynamic properties of cardiac sodium-calcium exchange. Ion and voltage dependencies of the transport cycle. *J. Gen. Physiol.* 100:963–1001.

Matsuoka, S., D.A. Nicoll, L.V. Hryshko, D.O. Levitsky, J.N. Weiss, and K.D. Philipson. 1995. Regulation of the cardiac Na^+-Ca^{2+} exchanger by Ca^{2+}: mutational analysis of the Ca^{2+}-binding domain. *J. Gen. Physiol.* 105:403–420.

Matsuoka, S., D.A. Nicoll, R.F. Reilly, D.W. Hilgemann, and K.D. Philipson. 1993. Initial localization of regulatory regions of the cardiac sarcolemmal Na^+-Ca^{2+} exchanger. *Proc. Natl. Acad. Sci. USA.* 90:3870–3874.

Nicoll, D.A., L.V. Hryshko, S. Matsuoka, J.S. Frank, and K.D. Philipson. 1996. Mutation of amino acid residues in the putative transmembrane segments of the cardiac sarcolemmal Na^+-Ca^{2+} exchanger. *J. Biol. Chem.* 271:13385–13391.

Nicoll, D.A., S. Longoni, and K.D. Philipson. 1990. Molecular cloning and functional expression of the cardiac sarcolemmal Na^+-Ca^{2+} exchanger. *Science (Wash. DC).* 250:562–565.

Niggli, E., and W.J. Lederer. 1991. Molecular operations of the sodium-calcium exchanger revealed by conformation currents. *Nature (Lond.).* 349:621–624.

White, M.M., and M. Aylwin. 1990. Niflumic and flufenamic acids are potent reversible blockers of Ca^{2+}-activated Cl^- channels in *Xenopus* oocytes. *Mol. Pharmacol.* 37:720–724.